Proton Induced X-ray Emission – A tool for non-destructive trace element analysis

I. M. Govil

Physics Department, Panjab University, Chandigarh 160 014, India

The paper describes the basic principle of the Proton Induced X-ray Emission (PIXE) technique for the trace element analysis. The use of this technique depends on the X-ray production cross-section, the fluorescence yield and the background radiation for a particular energy of the proton beam. The details for the sample preparation, high resolution X-ray detector and the multi-target vacuum chamber required for this purpose are given. The application of this technique for trace element analysis of aerosol, biological, archaeological, geological and medical samples are discussed.

1. Introduction

X-RAYS were first discovered by Roentgen[1] in the year 1895 during his experiment with cathode rays. The first Nobel Prize was awarded to Roentgen in 1901 for this remarkable discovery. The phenomenon of X-ray emission by heavy ions, i.e. alpha-particles from radioactive sources was reported by Chadwick[2] in 1912. The use of charged particle beams like protons[3], alpha particles[4] and other heavy ions from accelerators as a means of characteristic X-ray production for non-destructive trace element analysis in a large variety of materials including biological and environmental samples has received considerable attention in recent years[5–7]. The Proton Induced X-ray Emission (PIXE) has the advantage that the cross section for X-ray production is large and the background contribution from bremsstrahlung is low. Garcia *et al.*[8] have reported on the possibility of using heavy ions for X-ray production. It was found that there were some advantages over light projectiles, such as those due to the higher cross-sections available and the possibility of observing trace elements in high Z matrices. However, the heavy ions produce rather complicated X-ray spectra and for this reason this method was unlikely to have much application as a general-purpose multi-elemental analytical technique.

Johansson *et al.*[9] by making use of the high resolution Si(Li) photon detector and using MeV proton beams, showed that PIXE is a highly sensitive method for the multi-elemental analysis. They demonstrated that many elements could be detected simultaneously at the 10^{-12} g level. From that time, numerous reports have illustrated the fact that the concentrations of various elements with atomic number as low as 12 can easily be analysed in the ppm range. The need for a rapid non-destructive multi-elemental technique which probes the surface and near-surface region of materials has become apparent in fields of application as diverse as the semiconductor and corrosion industries as well as in biological, environmental, geological, metallurgical, archaeological and forensic sciences.

PIXE analysis consists of two parts. The first is to identify the atomic species in the target from the energies of the characteristic peaks in the X-ray emission spectrum and the second part is to determine the amount of a particular element present in the target from the intensity of its characteristic X-ray emission spectrum. This normally requires knowledge of the ionisation cross-sections, fluorescence yields and absorption coefficients. Depth profile analysis may be performed if the PIXE is combined with other methods like Rutherford Back Scattering (RBS) and/or sample etching techniques.

2. The basic principle of PIXE

X-rays may be produced following the excitation of target atoms induced by an energetic incident ion beam of protons or alpha particles as shown in Figure 1. The incident ions themselves may undergo further elastic or inelastic scattering during the collision. The excited target atom seeks to regain a stable energy state by reverting to its original electron configuration. In doing so, the electronic transition, which takes place, may be accompanied by emission of electromagnetic radiation in the form of X-rays characteristic of the excited atom. The emission consists of K, L, M,... lines produced by electron transitions to the K, L, M,... shells of the target atom. Hence, elemental composition analysis can be accomplished by determining the X-ray emissions emanating from the excited sample. Figure 2 shows schematically the consequences following charged particle ionization. Either an X-ray photon is emitted or electron emission can take place. The processes involved following ionization of the atom are illustrated schematically

in Figure 2*a–d*. The probability for X-ray emission is measured by the fluorescence yield parameter, ω, which increased gradually with atomic number *Z*.

2.1 *X-ray production cross-section*

For any measurement of an absolute nature to be made for PIXE analysis, the cross-sections for X-ray production σ_s^x (also known as X-ray emission cross-section s-shell index) rather than the ionization cross-section σ_s^i, must be known with some accuracy. The X-ray production cross-section σ_s^x for a K shell radiative transition is given by:

$$\sigma_K^x = \sigma_K^{(i)} \omega_K k,$$

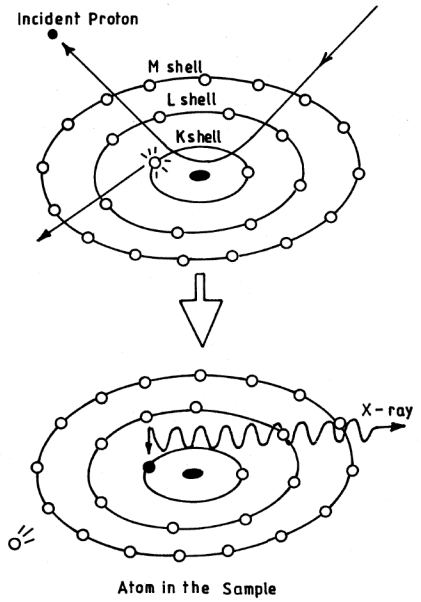

Figure 1. The basic principle of PIXE.

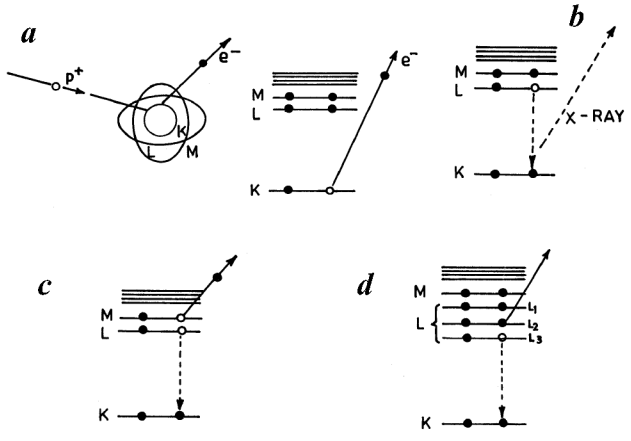

Figure 2. Ionization following charged particle bombardment and its consequences. ***a***, k-shell ionization; ***b***, X-ray emission; ***c***, Auger electrons; ***d***, Coster–Kroning transitions.

where $\sigma_K^{(i)}$ is the ionization cross-section for K-shell, ω_K is the fluorescence yield and k is the relative X-ray transition probability.

The total X-ray yield from an excited target atom is affected by the competing processes of the Auger and Coster–Kronig transitions. Auger transition is an auto-ionization process that arises from the electrostatic interaction between two electrons in an atom that is initially singly ionized in an inner shell. The vacancies which are created move towards the outer shells where they may create X-rays and Auger or Coster–Kronig electrons. The Auger process is illustrated schematically in Figure 2 *c*. Here the energy associated with the X-ray gets utilized to create vacancies by ejecting electrons from higher atomic shells. These are the Auger electrons. While the initial characteristic X-ray is 'lost', a higher order (for example L or M shell) characteristic X-ray may be emitted during the electron re-ordering process that takes place after the emission of the Auger electron. The Coster–Kronig effect takes place, although not for the K shell, through transitions between the subshells of an atomic shell having the same principal quantum number[10,11]. Hence, a primary vacancy created in one of the subshells can shift to a higher subshell before the vacancy is filled by another transition as shown in Figure 2 *d*. These competitive effects to characteristic X-ray emission are described by a factor called the fluorescence yield which may be defined as the ratio of emitted X-ray intensity due to transition to a particular shell and the number of primary vacancies created in that shell.

The derivation of the X-ray production cross-section σ^x is further complicated by the fact that radiative transitions to a particular energy level give rise to the emission of more than one X-ray line since the transitions can arise from different initial energy states. For example, the L X-ray emission is composed of X-rays originating from a multiplicity of transitions: $L_{\alpha 1}$, $L_{\alpha 2}$, $L_{\beta 1}$, $L_{\beta 2}$, $L_{\beta 3}$, ... all emitted with different intensities. Similarly, K-X-ray emission is composed of K_α and K_β lines. The fraction of a specific X-ray line emitted with respect to the total number of X-rays emitted from that shell is referred to as the relative X-ray transition probability, *k*.

2.2 *Background radiation*

The X-ray signal from the trace elements of interest may be partially or totally masked by an unwanted background marked A in the spectrum arising from the backing or host material. The background may be in the form of a continuum due to bremsstrahlung or it may contain discrete peaks arising from interfering characteristic X-rays from the matrix material. Figure 3 shows a typical X-ray spectrum obtained with a Si(Li) detector

when 1.5 MeV protons are incident on a thin carbon foil. It may be seen, that several discrete peaks are seen sitting on a continuous distribution which has a maximum at low energies. The decrease in the continuum at the lowest energies is due to absorption of X-rays in the Be window in front of the Si(Li) detector. The background at low energies prevents easy and precise analysis of the light elements in the spectrum. The main processes which contribute to the background are:

(i) Incident projectile bremsstrahlung. The background is illustrated in Figure 3 by the line marked B and would appear to be the major cause of background at high X-ray energies.

(ii) Secondary electron bremsstrahlung. The low energy background is believed to be largely due to the bremsstrahlung caused by the secondary electrons ejected from the target atoms during the collision process. The arrow marked at C in Figure 3 indicates the maximum secondary electron energy for 1.5 MeV protons. This energy increases with incident proton energy.

(iii) Low energy γ-rays. When a projectile is involved in a nuclear reaction, of a type such as (p, γ) or (α, γ) with a target, γ-radiation may be emitted which will produce a high energy tail in the spectrum due to Compton scattering in the detector. Moreover, if the γ-rays are of low energy, they may be directly detected in the detector and give rise to discrete peaks which may be mistaken for characteristic X-ray peaks. The γ-radiation produced depends on the projectile energy and to a high degree on the elemental composition of the target matrix.

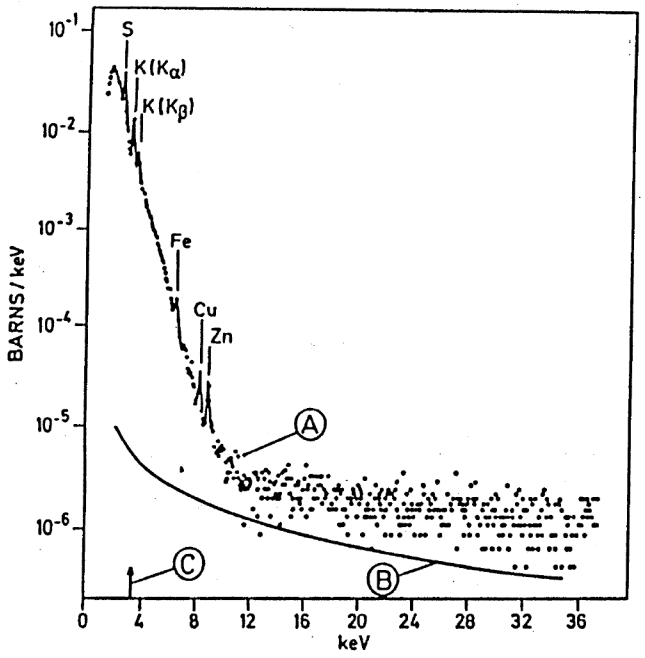

Figure 3. Spectrum of thin carbon foil bombarded with 1.5 MeV protons (for A, B, C see text). (Reprinted from *Nucl. Instrum. Methods*, Volume number 137, Johansson, S. A. E. and Johansson, T. B., Analytical application of particle induced X-ray emission, p. 473, Copyright (1976), with permission from Elsevier Science.)

3. Experimental considerations

In view of the rapid, non-destructive and multi-elemental nature of the PIXE method, much thought and care must go into the consideration of the experimental procedure. Figure 4 shows the experimental set up for PIXE analysis, which consists of the following parts.

3.1 *Vacuum chamber for sample irradiation*

This may be a steel or aluminium chamber of simple design with facilities for multi-target manipulation and transfer. The X-ray detector should be placed close to the target to provide a large solid angle. Sufficient space must be provided in the vacuum chamber for beam current measurements and for absorbers to be placed in front of the detectors and for any radioactive sources that may be necessary for calibration purposes. A practical example of the target chamber designed to contain a variety of targets and detectors is shown in Figure 4. For typical PIXE analysis, vacuum pressures of 10^{-3} torr are sufficient and this is easily achievable with a variety of vacuum pumps commercially available, although it is advisable to use the type of pumps that do not contaminate the specimen with backstreaming oil vapours.

3.2 *Non-vacuum irradiation*

The main incentive for non-vacuum irradiation studies lies in examining liquid and biological materials. These normally contain large amounts of water and volatile substances. The projectile beam normally exits the vacuum system via a thin foil window (which can, for example, be of mylar, nickel or beryllium) and the sample, together with the X-ray detection system, is situated in air or helium environment. There are two main advantages in the use of helium; first it is an inert gas and second, the stopping cross-section for the projectile beam in helium is about four times lower than in the case of air.

3.3 *Ion beam current measurements*

The ion beam intensity required for quantitative and semi-quantitative analysis and for normalizing between sequential irradiations is often determined by beam charge measurements. The ion beam current integration which is used to obtain the charge is either made by measuring the current on the (conducting) target itself

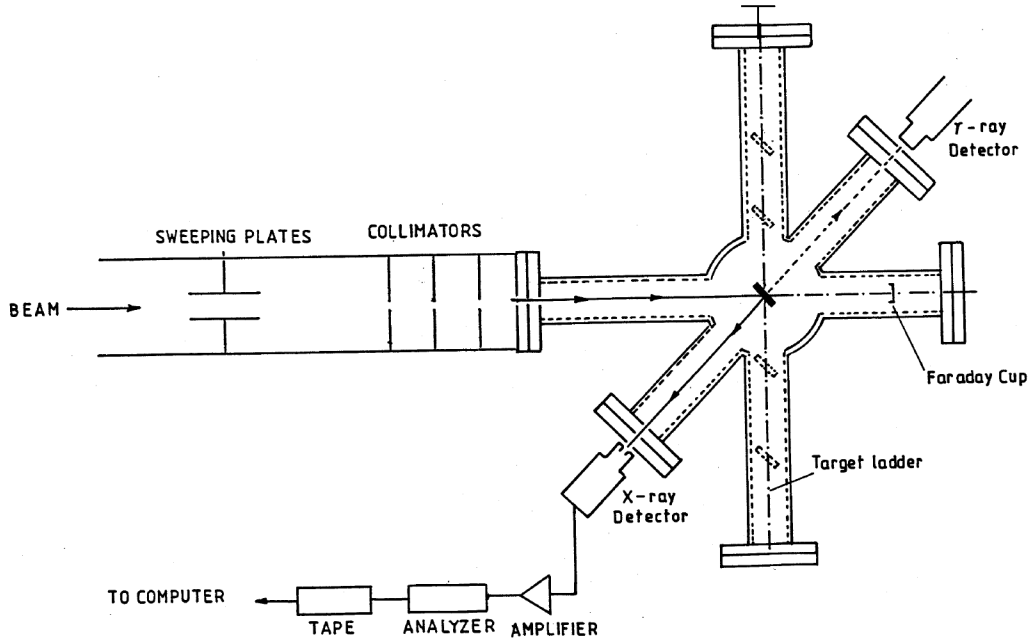

Figure 4. Schematic diagram showing the basic experimental arrangement and target chamber of a PIXE set-up.

or through the target (if it is thin enough to transmit the beam) into a Faraday cup behind it. For insulating targets the beam current may be measured by evaporating or coating a thin layer of conducting carbon layer on the front surface of the target or mixing of the specpure graphite powder in the target material in a predetermined quantity.

3.4 *X-ray detector*

It was only when Si(Li) X-ray detector became available in the late 1960s with resolutions of about 150 ev sufficient to distinguish between the X-rays of adjacent elements that rapid, non-destructive multi-elemental PIXE analysis became realizable. If absolute quantitative analysis is to be performed, the detector efficiency must be known accurately over an energy range sufficiently large to encompass all typically encountered characteristic X-ray energies.

Figure 5 *a* illustrates theoretical detector efficiency for a typical Si(Li) detector as a function of Be window thickness and silicon diode thickness for 0.1 to 100 keV energy. Figure 5 *b* illustrates the energy region from 1–10 keV. For accurate analysis, however, the detector efficiency for the specific Si(Li) detector used should be experimentally deduced. For energies above about 5 keV, this is achieved by using standard thin radioactive sources. High-count rates of X-rays in the detector can lead to an overloading of the electronics with resulting pile-up and electronic dead-time correction problems. Another aspect of a high-count rate is that it worsens the resolution and may cause peak shifting towards lower energies. It often happens that trace elements of interest are in sample matrices of a predominantly lower atomic number or, as is often the case in aerosol and dust studies, the trace elements are masked by a large peak of a minor component element, such as sulphur. These low Z elements can give very high count rates with all unwanted consequences mentioned earlier. A reasonable solution to this problem is the so-called 'funny filter' originally described by Harrison and Eldred and recently discussed extensively by Cahill[12]. An absorber of 30 mg cm^{-2} Kapton is placed in front of the detector. In the centre of this absorber, a hole is made of area about one-tenth of the detector active area. Consequently, the intensity of low energy X-rays is greatly reduced due to smaller solid angle available, whilst still permitting a sufficient number to pass through the hole and get detected by the detector with a reasonable count rate. The heavier trace elements, X-rays are mostly unaffected by the interposition of the absorber due to their relatively greater energies.

3.5 *Absorption of ions and X-rays in the sample*

In case of thin targets where the projectile beam loses little or no energy in the specimen, the characteristic X-rays emitted are not attenuated in the exit path from the target. This, however, is not the case for thick targets. In thick samples, the projectile ions lose energy in penetrating the target, finally coming to rest in the material at some distance from the surface. The characteristic X-rays are generated over the total path of the

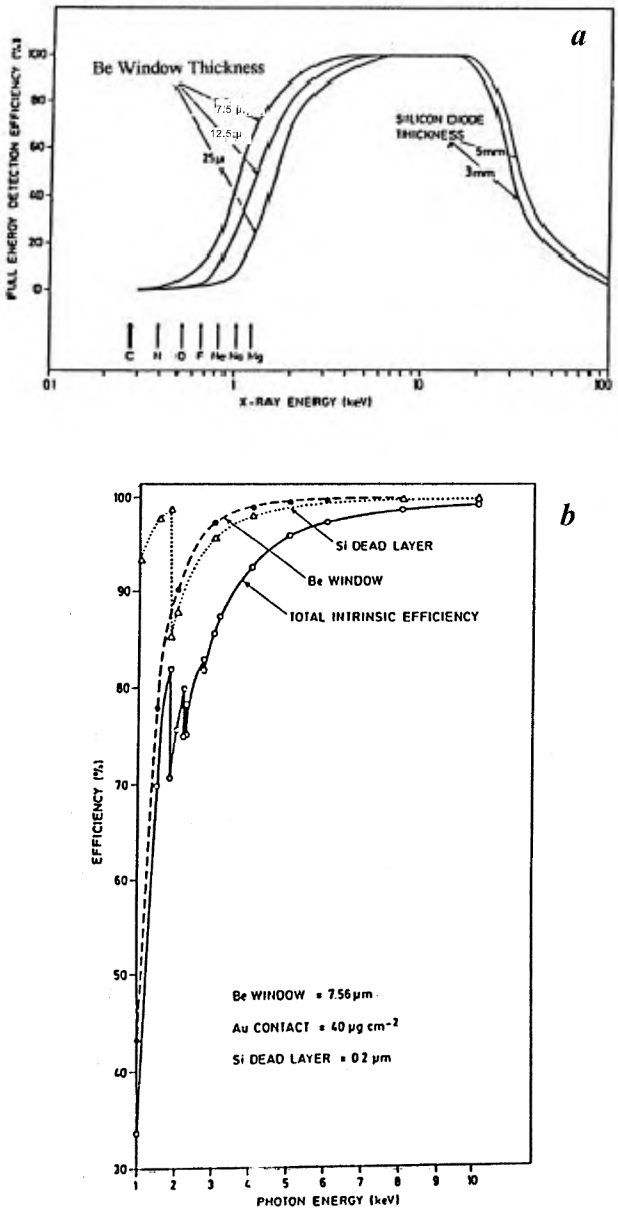

Figure 5. *a*, Detection efficiency of a Si(Li) detector from 0.1 to 100 keV; *b*, Detection efficiency of a Si(Li) detector from 1 to 10 keV including corrections due to absorber layers.

projectile in the sample and must reach the target surface before being detected. Since the cross-section for X-ray production varies with projectile energy, it becomes necessary to integrate the X-ray production yield over the total projectile path length. This requires a knowledge of the variation with energy of X-ray production cross-sections and the stopping cross-sections of the projectile in the matrix.

3.6 *Target preparation*

For many types of samples, a backing substrate is often necessary. The latter may possess high mechanical strength, good electrical and thermal conductivity, high purity, resistance to high beam intensities and non-reactivity with the target material itself. The background continuum produced by the substrate should be as low as possible and this favours thin backings composed of low Z elements which will produce less secondary electron and proton bremsstrahlung. The substrates of carbon, beryllium, boron or plastic-like materials are generally used. Characteristic X-rays due to the substrate will be detected less as most of these will be absorbed by the beryllium detector window and intervening absorbers.

3.7 *Data analysis*

The analysis of PIXE spectrum presents little difficulties when a sample contains only a few elements. However, in many practical situations such as in the analysis of environmental samples, a multitude of trace and minor component elements can be present. Each of these elements may give rise to one or more X-ray peaks due to the K, L and M shell transitions, subdivided to give peaks corresponding to K_α, K_β, L_α, L_β, L_γ etc. some of which are capable of being resolved. Thus a large number of both large and small peaks can be expected in such environmental samples. There is a high probability that a number of the X-ray peaks will be overlapping and interfering with each other. This can make data reduction and interpretation complicated. Even when the number of samples to be analysed is small, the use of a computer programme to unravel overlapping peaks is often useful. When routine analyses are to be performed on a variety of samples of differing compositions, a spectral analysis programme is essential. Several programmes[13,14] and Gupix computer code[15] are useful for this purpose.

3.8 *Microprobe*

Properties of many materials are often dependent on the spatial distribution and concentrations of the component elements present in a matrix. In recent years considerable interest has been generated in producing spatially sensitive particle micro beams. Proton beam diameter as small as 2 μm by magnetic focussing has been reported by Cookson *et al.*[16]. Augustyniak[17] and Krejcik *et al.*[18] have reported microbeams of 15 μm and 40 μm respectively by electrostatic focussing.

3.9 *High energy PIXE*

High energy protons 20–25 MeV are useful for detection of trace elements in rare earth region due to their high K X-ray ionisation cross-section. Figure 6 *a* shows a typical X-ray spectrum obtained by our group[19] with

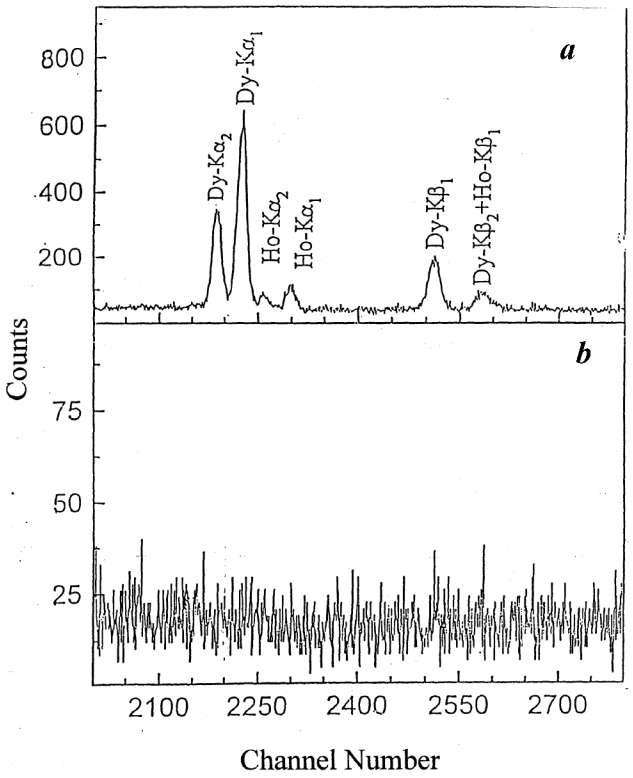

Figure 6. *a*, PIXE spectrum on Dy Target at E_p = 25 MeV; *b*, the background spectrum without the target. (Reprinted from *Nucl. Instrum. Methods*, Volume number B160, Hajivaliei, M. *et al.*, K and L X-ray production cross section and intensity ratios of rare-earth elements for proton impact in the energy range 20–25 MeV, p. 203, Copyright (2000), with permission from Elsevier Science).

25 MeV proton beam available from 15 UD Pelletron at the Nuclear Science Centre (NSC), New Delhi. The Dysporsium (Dy) K_α peaks are clearly visible in the spectrum. The Holmium K_α and K_β peaks seen in the figure are due to the Holmium nuclei produced due to (p, n) reaction at these energies. Figure 6 *b* shows the background spectrum without the target.

3.10 *Heavy ion PIXE*

Heavy ion induced X-ray spectra are in general more complex than equivalent light ion spectrum. Though the spectrum complexity and larger bremsstrahlung backgrounds act against the use of heavy ions, since the mean range of these ions is small compared with light ions, this technique may prove to be useful in surface layer analysis. Chemin *et al.*[20] have shown that fractions of a monolayer may be detected in this way.

4. Applications

4.1 *Aerosol studies*

In recent years, many governments and a number of international agencies have been increasingly concerned by the gradual erosion of the quality of the environment by all manner of industrial, man-made and natural pollutants. Environmental quality investigations have indicated that, due to the small samples generally available and the low toxic levels often involved, there is a need for highly sensitive multi-elemental analysis procedures capable of ready application to air, water, soil and biological samples. In particular, concern about the harmful effects of air pollution has stimulated an interest in the origin, conversion and eventual dispersal of particulate matter in the environment. The PIXE technique has shown itself well suited to precisely this type of broad range analysis, covering almost the entire spectrum of elements whilst requiring only micrograms of total samples. Studies of airborne contamination using PIXE and related techniques have been undertaken by several laboratories around the world and they clearly demonstrate its value in environmental sciences. Figure 7 *a* shows a typical PIXE spectrum taken at IOP, Bhubaneswar[21] of an aerosol sample from Chandigarh and Figure 7 *b* the background spectrum from the blank filter on which the sample was collected.

4.2 *Biological studies*

Considerable efforts expended in the past ten years in the development of PIXE has been in investigating bio-

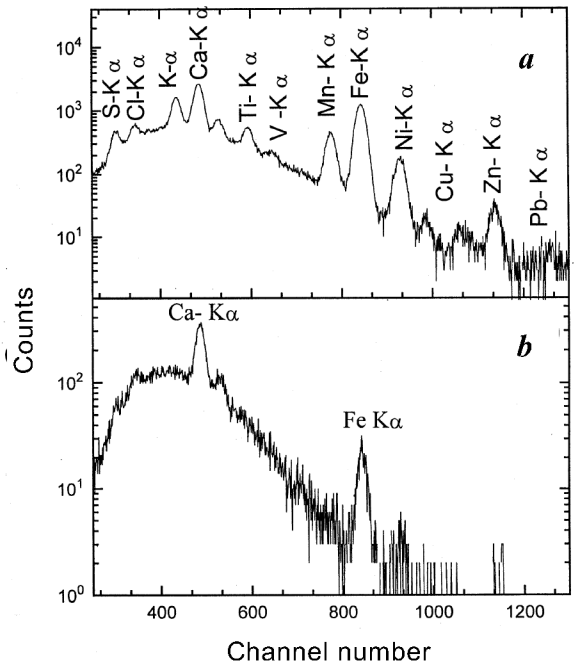

Figure 7. *a*, A typical PIXE spectrum of an aerosol sample of Chandigarh; *b*, the background spectrum from blank filter. (Reprinted from *Nucl. Instrum. Methods*, Volume number B160, Bandhu, H. K. *et al.*, Elemental composition and sources of air pollution in the city of Chandigarh, India, using EDXRF and PIXE techniques, p. 126, Copyright (2000), with permission from Elsevier Science.)

logical and medical samples. This arises not only because of the versatility and ease with which PIXE can be used to obtain quantitative and multi-elemental information on small samples but also because of the non-destructive nature of the technique with minimal beam-induced effects on the specimen itself, as compared with more classical physical and chemical analysing methods. Trace elements have an important function in biological systems and the various concentrations play an important part in diagnosis of diseases. For example, many clinical and pathological disorders arise in animals and men as a consequence of trace element deficiencies or excesses. Lear *et al.*[22] investigated cadmium concentrations in kidney and found a correlation with age and the state of the disease under study. Figure 8 shows the spectrum of the kidney stone which indicates presence of trace elements of Ti, Mn, Fe, Cu and Zn beside the main peak of calcium corresponding to calcium oxalate present in the stones. The trace element present varied with age, sex and dietary habits of the patients from a particular region. PIXE has been extensively used for the analysis of hair[23], blood serum[24] and saliva samples[25]. This has also been used for trace element analysis in diseased plants like apples etc.[26].

4.3 *Archaeological studies*

It is often difficult to prepare PIXE targets in the form of thin samples. In these cases thick samples of the specimens of interest may sometimes be used. As for instance, a thick section of tissue, bone, rock or archaeological sample may be mounted and irradiated

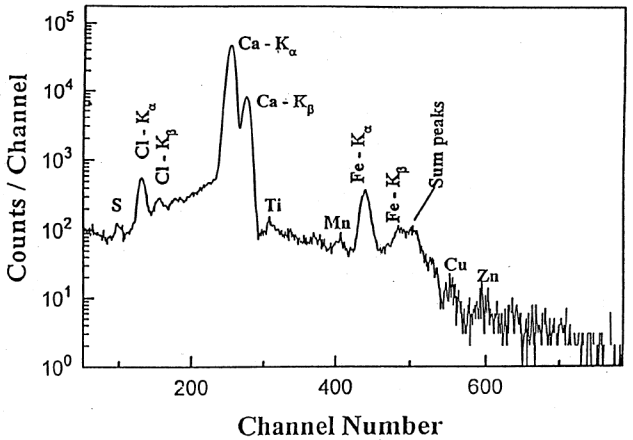

Figure 8. PIXE spectrum of kidney stone (belonging to 60 years old male).

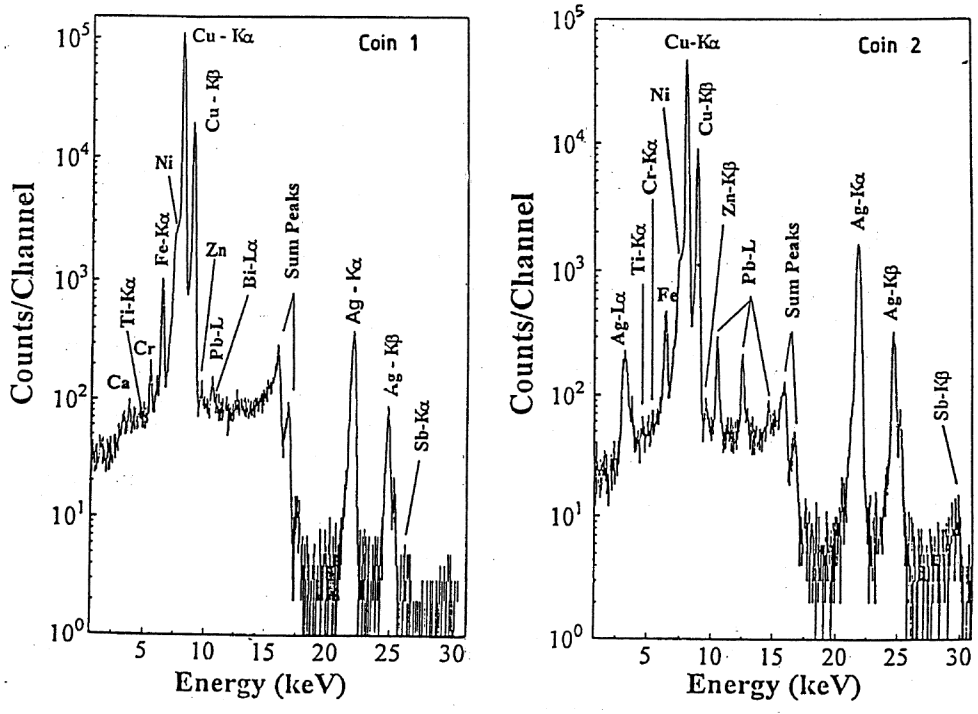

Figure 9. PIXE spectrum of ancient Indian coins of Hindu Sahi Dynasty (990–1015 AD). (Reprinted from *Nucl. Instrum. Methods*, Volume number B150, Hajivaliei, M. *et al.*, PIXE analysis of ancient Indian coins, p. 645, Copyright (2000), with permission from Elsevier Science.)

directly, either in vacuum or in a non-vacuum facility, with no pretreatment or further preparation being necessary. However in some cases a pretreatment may be necessary to clean dust, rust and corrosion products on the surface. PIXE studies have found great use in archaeological and numismatic studies. The trace element analysis of an archaeological artifact (an ancient coin) provides information about its origin. Figure 9 shows PIXE spectrum of the ancient Indian coins[27] of Hindu Sahi dynasty (990–1015 AD). These coins are made mainly of Cu and Ag. The presence of trace element like Ti, Cr, Ni, Fe, Bi and Pb provides information about the source of copper (Khetri mines in Rajasthan) and silver (Afghanistan). Chen *et al.*[28] have reported the trace element analysis of precious archaeological sword samples which were more than 2500 years old.

4.4 *Geological studies*

Cohen *et al.*[29] reported on the application of PIXE for measurement of thorium and uranium at the ppm level in thick ore samples, which has important practical implications in the mining industry. PIXE analyses on mineral monazite samples from Malaysia and various monazite inclusions in biotite mica have been carried out in a project designed to search for the presence of the superheavy elements[30]. All manner of ore, coal and rock samples[31] have been studied for their trace element contents and even meteoritic and lunar samples have been successfully treated in this way. Van Grieken *et al.*[32] using very small samples, measured the zirconium–hafnium ratio of geological samples of zircon.

5. Conclusion

PIXE within a short span of time has demonstrated its versatility and usefulness by the diversity of applications to which it has been applied. The results obtained indicate that it is competitive with other more classical analytical methods, and that it may be, in addition, a very useful complementary technique when combined with other ion beam methods. PIXE is capable of multi-elemental analysis and a large number of elements may be seen simultaneously. The method is a very sensitive one having a minimum detectable concentration of about 0.1–1 ppm under optimum conditions. In principle, PIXE, being a non-destructive technique and because the original shape and size of the sample is not destroyed, makes it a unique facility for a number of applications[33].

In the coming years PIXE should find itself being applied more and more to a variety of samples, when a rapid non-destructive and multi-elemental method is looked for, and it should take its rightful place as an equal or better technique among the numerous other standard analytical techniques available.

1. Roentgen, W. C. Sitzungsber. dev Wurgburgev Physik-Medic, Gesellsch, Jahrg. 1895, *Ann. Dev. Phys.*, 1898, **64**, 1.
2. Chadwick, J., *Phil. Mag.*, 1912, **24**, 594.
3. Johansson, S. A. E. and Johansson, T. B., *Nucl. Instrum. Methods*, 1976, **137**, 473.
4. Watson, R. L., Sjurseht, J. R. and Howard, R. W., *Nucl. Instrum. Methods*, 1971, **93**, 69.
5. Folkmann, F., Gaarde, C., Huust, T. and Kemp, K., *Nucl. Instrum. Methods*, 1974, **116**, 487.
6. Lear, R. D., Van Rinsvelt, H. A. and Adams, W. R., *IEEE*, 1977, **93**, 1175–1179.
7. Walter, R. L., Willis, R. D., Gutkneck, W. M. and Joyce, J. M., *Anal. Chem.*, 1974, **46**, 843.
8. Garcia, J. D., Fortner, R. J. and Kavanagh, T. M., *Rev. Mod. Phys.*, 1973, **45**, 111.
9. Johansson, T. B., Akselsson, R. and Johansson, S. A. E., *Nucl. Instrum. Methods*, 1970, **84**, 141.
10. Puri, S., Mehta, D., Chand, B., Singh, N. and Trehan, P. N., *X-ray Spectro.*, 1993, **22**, 358.
11. Puri, S., Mehta, D., Chand, B., Singh, N. and Trehan, P. N., *Nucl. Instrum. Methods*, 1993, **B83**, 21.
12. Cahill, T. A. (ed. Ziegler, J. F.), Plenum Press, New York, 1975, p. 19.
13. Nass, M. J., Lurio, A. and Ziegler, J. F., *Nucl. Instrum. Methods*, 1978, **154**, 567.
14. Von Espen, R., Nullens, H. and Adams, F., *Nucl. Instrum. Methods*, 1977, **142**, 243.
15. Maxwell, J. A., Teesdale, W. J. and Campbell, J. L., *Nucl. Instrum. Methods*, 1995, **B95**, 407.
16. Cookson, J. A., *Nucl. Instrum. Methods*, 1979, **165**, 477.
17. Augustyniak, W. M., Betteridge, D. and Brown, W. L., *Nucl. Instum Methods*, 1978, **149**, 669.
18. Krejcik, P., Delglish, R. L. and Kelly, J. C., *J. Phys.*, 1979, **D12**, 161.
19. Hajivaliei, M., Puri, Sanjiv, Garg, M. L., Mehta, D., Kumar, A., Chamoli, S. K., Avasthi, D. K., Mandal, A., Nandi, T. K., Singh, K. P., Singh Nirmal and Govil, I. M., *Nucl. Instrum. Methods Phys. Res.*, 2000, **B160**, 203.
20. Chemin, J. F., Mitchell, I. V. and Saris, F. W., *J. Appl. Phys.*, 1974, **45**, 532.
21. Bandhu, H. K., Puri Sanjiv, Garg, M. L., Singh, B., Shahi, J. S., Mehta, D., Swietlicki, E., Dhawan, D. K., Mangal, P. C. and Singh Nirmal, *Nucl. Instrum. Methods Phys. Res.*, 2000, **B160**, 126.
22. Lear, R. D., Van Rinsvelt, H. A. and Adams, W. R., *Adv. X-ray Anal.*, 1976, **19**, 521.
23. Montenegro, E. C., Baptista, G. B., de Castro Faria, L. V. and Pashoa, A. S., *Nucl. Instrum. Methods*, 1980, **168**, 479.
24. Lecomte, R., Paradis, P., Monaro, S., Barrette, M., Lamoureuxm G. and Menard, H. A., *Nucl. Instrum. Methods*, 1978, **150**, 289.
25. Valcovic, V., *Nucl. Instrum. Methods*, 1977, **142**, 151.
26. Meyer, B. R. and Boulle, G. J., *J. South African Atomic Energy Board*, July 1978.
27. Hajivaliei, M., Garg, M. L., Handa, D. K., Govil, K. L., Kakavand, T., Vijayan, V. Singh, K. P. and Govil, I. M., *Nucl. Instrum. Methods Phys. Res.*, 1999, **B150**, 645.
28. Chen, Jian-Xin, Li, Hong-Kou, Ren. Chi-Gang and Yang Fu-Chia, *Nucl. Instrum. Methods*, 1980, **168**, 437.
29. Cohen, D. D., Duerden, P., Clayton, E. and Wall, T., *Nucl. Instrum. Methods*, 1980, **168**, 523.
30. Gentry, R. V., Cahill, T. A., Fletcher, N. R., Kaufmann, H. C., Medsker, L. R., Neslon, J. W. and Flocchini, R. G., *Phys. Rev. Lett.*, 1976, **37**, 11.
31. Clark, G. F., *Nucl. Instrum. Methods*, 1980, **168**, 125.
32. Van Grieken, R. E., Johansson, T. B., Winchester, J. W. and Odom, L. A., *Z. Anal. Chem.*, 1975, **275**, 343.
33. Mitchell, I. V. and Barfoot, K. M., *Nuclear Science Application*, Harvard Academic Press, UK, 1981, p. 99.